

Comparison of Fur and Lark diatomite potential for hydrocarbon production and CO₂ storage.

Veronika Abdulina^{1,*}, Aleksandr Mamonov², Skule Strand¹, and Tina Puntervold¹

¹ Department of Energy Resources, Faculty of Science and Technology, University of Stavanger, 4036 Stavanger, Norway

² Danish Offshore Technology Centre, Danmarks Tekniske Universitet, DK-2800 Kgs. Lyngby, Denmark

Abstract. Diatomite rock samples were compared and evaluated with respect to their hydrocarbon production and CO₂ storage potential. Samples of diatomite reservoir rock from the Norwegian Continental Shelf and diatomite outcrop rock from the Fur formation in Denmark were compared using a series of solid and surface characterization techniques. The results of this comparison study showed that Fur outcrop diatomite consists almost entirely of opal, while the Lark reservoir diatomite, in addition to opal, contains various clay minerals, mica and pyrite. Due to large differences in mineralogical composition, the physicochemical behaviour of Fur outcrop diatomite is not directly comparable to that of the Lark reservoir diatomite. This observation suggests that results obtained by laboratory tests performed on Fur outcrop diatomite are not directly transferable to reservoir behaviour. However, since the tests showed very high purity of the Fur outcrop material (approximately 98% of opal), this diatomite can be used to investigate pure diatomite surface reactivity and wettability behaviour. Spontaneous imbibition tests with formation water performed on a Fur diatomite rock sample showed 75% of oil recovery, consistent with a strongly water-wet behaviour. It was found that both the reservoir and the outcrop diatomite possessed high porosity, about 50% and 70%, respectively, and low permeability, about 0.2 mD and 6.8 mD, respectively. Thus, reservoir diatomite from the Lark formation and outcrop diatomite from the Fur formation can be considered suitable for geological storage of CO₂.

1 Introduction

The Norwegian Offshore Directorate has categorized reservoirs with permeabilities below 10 mD as tight reservoirs [1]. Within this category fall both chalk (carbonate) and diatomite reservoirs. Chalk reservoirs, such as the fractured Ekofisk field, on the Norwegian Continental Shelf (NCS) are well-known and have been developed and successfully produced by waterflooding since the 1980's [2]. Diatomite is a relatively rare type of reservoir rock, both on the NCS and globally, and has therefore been less studied compared to carbonates and sandstones. Diatomite is a silicious material of biogenic origin, which can be characterized by high porosity (>50%) and low permeability, thus it has a great potential for containing large volumes of hydrocarbons and storing great amounts of gases, such as CO₂ or H₂. Oil recovery from low permeability and high porosity diatomaceous reservoir rocks has been performed for several decades in the USA, e.g. in the Lost Hills field in California [3]. A CO₂ injection pilot was also performed in the Lost Hills field in the late 1990's – early 2000's. For 3 years the pilot project had excessive sand production and did not manage to overcome the operational problems. CO₂ injection appeared to be the reason for the sand problems, and it

was concluded that the Lost Hills field was not appropriate for CO₂ storage [4, 5].

In porous rock systems of low permeability, pore throat sizes are generally small, which results in high capillary pressure (P_c) between oil and water according to the Young-Laplace equation:

$$P_c = \frac{2\sigma\cos\theta}{r} \quad (1)$$

Where P_c is capillary pressure, σ is interfacial tension between oil and water, θ is the wetting angle through the water phase, and r is the radius of the pore throat of the porous media.

Capillary forces in a water-wet porous medium facilitate the spontaneous uptake of water into the pores and displacing the crude oil. Spontaneous imbibition of water into the pores is therefore an important driving mechanism for the oil displacement from low permeable diatomite material. Akin et al. (2000) observed that outcrop Lompoc diatomite from California, possessed strong capillary forces, caused by the water-wet behaviour of the rock [6]. Diatomite rocks can have varying mineralogical composition because of different depositional environments, and can also have local variations in physical properties, such as porosity, permeability, and surface area. These variations can

* Corresponding author: veronika.abdulina@uis.no

influence important reservoir rock and fluid properties such as wettability and fluid saturations, which again have impact on the location and flow characteristics of the in-situ fluids. Hence, to study reservoir rock behaviour and potential for hydrocarbon production and geological storage of CO₂ in the laboratory, in the lack of sufficient amount of reservoir material, one should ideally work with analogue outcrop rocks of similar mineralogy, containing comparable porosity and permeability characteristics.

In this work, various chemical analytical tools and methods such as Scanning Electron Microscopy (SEM), Energy-dispersive X-ray spectroscopy (EDX), X-ray powder diffraction (XRD), Mercury Injection Capillary Pressure (MICP) pore structure determination and Brunauer–Emmett–Teller (BET) surface area determination, were applied to characterize and compare the properties of a diatomite reservoir rock from the Lark formation on the NCS with those of a diatomite outcrop rock from the Fur formation, sampled in Denmark. These initial tests were performed to assess properties such as porosity and permeability, mineralogical composition, and surface area, all important for both hydrocarbon production and potential CO₂ storage. Spontaneous imbibition tests were performed to evaluate capillary forces, which are important for fluid displacement in tight rocks. Finally, both diatomite rocks were exposed to carbonated water (brine containing dissolved CO₂) to evaluate how the rock and minerals were affected by the exposure in the event diatomite formations are to be used for geological CO₂ storage. The obtained data provide an understanding of which oil recovery technologies to be deployed or developed for hydrocarbon production from reservoir diatomite rock. This initial work is part of a study to couple oil production and CO₂ storage through the use of carbonated Smart Water. This hybrid method benefits from wettability alteration and improved reservoir sweep by Smart Water, facilitated fluid flow by the presence of CO₂, and with the additional benefit of subsurface CO₂ storage.

2 Experimental materials and methods

2.1 Materials

2.1.1 Reservoir diatomite – reservoir diatomite (Norway)

The studied reservoir diatomite (RD) comes from the Lark formation on the NCS and was sampled from the core storage at The Norwegian Offshore Directorate (NOD). Visually, the samples were of greyish brown colour, odourless and well-compacted, massive but layered, and easily crushed (Figure 1).

2.1.2 Outcrop diatomite – outcrop diatomite (Denmark)

The studied outcrop diatomite (OD) comes from the Fur formation in Denmark. Visually, the samples were light-

greyish-white colour, laminated with white and grey layers, very light-weight and easily crushed (Figure 2).



Fig. 1. Reservoir diatomite from the Lark formation at the core storage of the Norwegian Offshore Directorate.



Fig. 2. Samples of outcrop diatomite from the Fur formation.

2.2 Methods

To compare the properties of the Norwegian reservoir diatomite with the Danish outcrop diatomite a combination of tests was performed. The following methods were used to determine the physical and chemical properties of the solid material:

- Scanning electron microscopy (SEM),
- Energy-dispersive X-ray spectroscopy (EDX),
- Mercury injection capillary pressure (MICP),
- Brunauer–Emmett–Teller (BET) surface area determination,
- X-ray powder diffraction (XRD),
- Ion chromatography (IC),
- Zeta-potential measurement.

Preparation of the diatomite samples for the SEM study followed standard laboratory techniques [7]. SEM was performed using a Zeiss Supra VP35 equipped with an EDX system. All the samples were coated with

palladium (30 nm thickness). The porosity and permeability were studied using MICP equipment - AutoPore IV 9500 V1.05. The BET surface area measurements were obtained using a Micromeritics TriStar II. The XRD patterns were obtained using a Bruker D8 Advance Eco diffractometer. To measure anion and cation concentrations in the brine during the exposure tests IC was performed using a DIONEX 5000. The zeta potential measurements were conducted with a Malvern Zetasizer Nano ZS.

2.2.1 Spontaneous imbibition

Spontaneous imbibition (SI) tests were carried out to study the wettability of the diatomitic samples (Table 1). First, the samples were mildly cleaned with a non-polar solvent (heptane, C₇H₁₆) and second by a 1000 ppm NaCl (low salinity – LS) brine (Table 2). This procedure was chosen to preserve the initial wettability of the diatomite samples [8]. Heptane was used to remove oil from the pore matrix, and LS was introduced to displace the heptane while preventing potential clay swelling.

Table 1. Samples parameters for SI tests.

Parameters	Reservoir diatomite	Outcrop diatomite
Shape	Rectangular parallelepiped	Cylinder
Length, mm	32.43	37.83
Width, mm	21.77	37.83
Height, mm	38.22	33.09
Weight (dry), g	30.02	21.27
Pore volume, ml	13.64	25.94
Porosity, %	48.6	68.7
%OOIP recovered during SI	45.01	75.38

After the cleaning procedure, the samples were dried in the oven at 90 °C. Then, the samples were vacuumed and saturated with fivefold diluted formation water – (FW) (Table 2). A desiccator was used to gradually dry the samples down to 20% of initial water saturation (S_{wi}). By this way, the residual brine inside the rocks had reached the original FW composition after desiccation [9]. Thereafter, the samples with $S_{wi} = 20\%$ were saturated with Varg oil (Table 3) for 24 hours.

The SI test is used to evaluate the wettability of a rock through the action of capillary forces. In this method, a restored sample is submerged in either water or oil within an Amott cell, as described by Amott in 1959 [10]. When the surrounding fluid matches the wetting phase of the system, it imbibes into the sample's pores, displacing the mobile in-situ fluid. The recovered crude oil was collected in a graded burette and the recovery factor, expressed as a percentage of original oil (%OOIP), was determined over

the duration of the imbibition test. SI experiments were conducted at room temperature using FW as the imbibing fluid.

Table 2. Brine properties and ion compositions in mM.

Ion	Low salinity water (LS)	Formation water (FW)
HCO ₃ ⁻	0	9.3
Cl ⁻	17.1	1066.1
Mg ²⁺	0	7.8
Ca ²⁺	0	28.9
Na ⁺	17.1	996.6
K ⁺	0	5.3
Ionic strength (M)	0.017	1.112
TDS (g/l)	1	62.83
Density (g/l)	1.001	1.024

Table 3. Varg oil properties.

Properties	Varg oil
Acid number (mg KOH/g)	0.13
Base number (mg KOH/g)	0.85
Density @ 20°C (g/cm ³)	0.842
Viscosity @ 20°C (cp)	8.6

2.2.2 CO₂ exposure tests

The exposure test procedure was the same as that described by Fani et al. [11]. Each rock sample was crushed using a ceramic mortar with a pestle. Then the samples were sieved through a 0.5 mm mesh and milled with deionized water (DI) for 10 min using a McCrone mill. Following a 24-hour oven drying process at 80 °C, the samples were again sieved through a 0.5 mm mesh and prepared for further tests. A 2 g powdered rock sample was placed in a sample stainless steel cup inside a sealed high-pressure, high-temperature stainless steel piston cell. Initially, 80 mL of CO₂ was injected into the cell at 15 bar pressure and room temperature. Next, 100 mL of LS brine were introduced into the cell to mix with the CO₂, elevating the test pressure to 80 bar. After reaching equilibrium, during which CO₂ partially dissolved in the water phase, carbonated low salinity (CLS) brine was produced. Subsequently, the exposure test cell with rock and fluid was placed in the oven to reach a temperature of 60 °C, allowing for the dissolution of CO₂ in water and facilitating fluid-rock interactions over time. The mineral

samples were exposed to carbonated water at pressure of 80 bar and temperature of 60 °C conditions for one month.

The interaction between brine, CO₂, and rock surface can lead to modifications in the brine composition. Therefore, the brine samples were extracted from the test cells throughout the whole exposure test to analyse the ion composition. Ion chromatography (IC) was used to measure the concentrations of anions and cations in the brine. Additional fluid samples were also collected for pH measurements.

At the end of the exposure test, the rock phase was extracted and prepared by drying and coating with palladium for high-resolution SEM images after the CO₂ exposure. Mineral grain shapes and any changes in grain boundaries, morphology, and surfaces were assessed by comparing the before and after images. EDX, in conjunction with SEM, was utilized to identify the elemental composition of the sample surfaces. The findings from this analysis were compared with images and assessments of the mineral samples in their original, unexposed state. This information was then used to evaluate the interactions between the brine and the rocks during exposure to CLS.

3 Results and discussion

3.1. Rock characterization

3.1.1 Reservoir diatomite – RD (Norway)

The diatomitic samples from the NCS are characterized with a mineralogical mixture. The cation atomic content was defined with SEM analysis (Figure 3) combined with EDX analysis (Table 4). The atomic content is based on the area of the SEM image, and thereafter, it can vary, depending on the chosen area of a sample. The dominant elements are silicon and aluminium. The quantitative detection of mineral phases, using XRD, is challenging since the samples contain an amorphous phase of silica oxide – opal. However, XRD defined the presence of muscovite, pyrite and some clay minerals: illite and kaolinite.

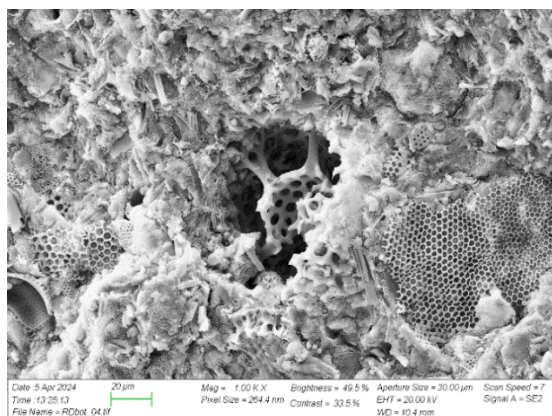


Fig. 3. SEM image of the cleaned reservoir diatomite at a magnification 1000.

To identify the porosity and permeability, MICP tests of the rock samples were performed. As it follows from the results (Table 4), the porosity of reservoir diatomite is quite high – around 50%, and the permeability is quite low – about 0.2 mD.

The surface area measurements were quantified by BET analysis. The reservoir diatomite is characterized with 23.4 m²/g surface area (Table 4). By zeta-potential measurements in DI, LS, and FW, the reservoir diatomite was found to have a negative charge (Table 4).

Table 4. Rock characteristics of reservoir diatomite and outcrop diatomite.

methods		Reservoir diatomite	Outcrop diatomite
EDS (atomic %)	Na	1	0
	Mg	1	0
	Al	16	2
	Si	59	98
	S	5	0
	K	9	0
	Fe	9	0
MICP	Porosity (%)	48.6	68.7
	Permeability (mD)	0.248	6.819
BET (m ² /g)		23.4	18.9
XRD		Opal Illite Kaolinite Muscovite Pyrite	Opal
Zeta-potential in DI*		-30.06 at pH 3.8	-14.68 at pH 5.2
Zeta-potential in LS*		-34.31 at pH 3.8	-33.96 at pH 4.7
Zeta-potential in FW*		-23.61 at pH 4.7	-21.45 at pH 6.7

*measured at room temperature

3.1.2 Outcrop diatomite – OD (Denmark)

Diatomite from the Fur formation in Denmark is a pure diatomitic rock. The SEM images show the rock surface, which consists of variously shaped diatoms (Figure 4). The SEM analysis combined with EDX analysis showed the cation percentage distribution – 94.31% of silicon and 5.69% of aluminium (Table 4). The mineralogical definition, using XRD, showed the pure amorphous phase – opal.

MICP tests showed that the outcrop diatomite samples are characterized with very high porosity – around 70%, and low permeability – 6.819 mD (Table 4).

The surface area measurements, quantified by BET analysis, showed quite a comparable to reservoir diatomite surface area – 18.9 m²/g (Table 4). Zeta-potential measurements in DI, LS and FW, outcrop diatomite was found to have a negative charge, as was observed for reservoir diatomite (Table 4).

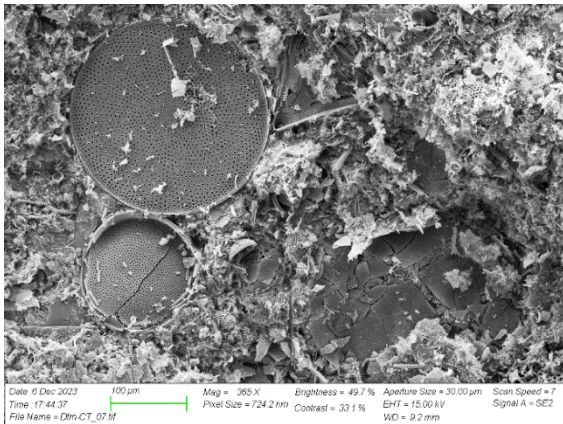


Fig. 4. SEM image of the cleaned outcrop Fur diatomite at magnification 365.

3.2 The comparison of hydrocarbon production potential

According to the BET analysis (Table 4), there is a large surface area available to interact with fluids. Nonetheless, the volume of formation water in reservoirs is quite small. Therefore, the rock-fluids interactions play a significant role in hydrocarbon production. An important surface property, which many researchers focus on, is wettability. The wettability alteration towards more water-wet conditions can improve hydrocarbon production during water injection into reservoirs [12-16].

One of the methods to calculate oil recovery during the water injection is spontaneous imbibition (SI) tests. These tests were performed on both the reservoir and outcrop diatomitic samples using FW as imbibing fluid. Since the sample preparation included saturation with FW, the rock surface and the fluids are already in equilibrium. Thus, the SI tests with FW will show the action of capillary forces within the porous structure of the sample without wettability modifications [16].

After using heptane and LS brine for cleaning purposes, the reservoir and outcrop samples were dried in the oven. After the samples were fully saturated with diluted FW, S_{wi} was decreased to 20%, using desiccator. Then the diatomitic samples were saturated with Varg oil for 1 day at the ambient temperature. Subsequent SI test with FW at the ambient temperature was performed to evaluate the mobilization of oil by positive capillary forces.

The results show that the outcrop diatomite is quite water-wet with an oil production of 72% OOIP obtained after 3 days of imbibition, reaching ultimate recovery of 75% OOIP after 8 days (Figure 5). This rapid imbibition behaviour indicates the action of strong capillary forces, which is consistent with the results obtained by Schembre et al. (1998) for outcrop Lompoc diatomite from California [17]. The reservoir rock reached an ultimate recovery of 45% OOIP after 8 days. The spontaneous imbibition process starts later in reservoir sample, and it is slower. As known, the mineralogy of the rock dictates its surface charge and ability for wettability alteration. For instance, higher content of clay minerals makes the rock surface less water-wet, since clays adsorb oil components.

It happens because of the crystal structure of clays which have permanent negative charges. This indicates that reservoir diatomite, which contains clay minerals that can influence the rock wettability [18], is mixed-wet, thus, the oil production proceeds slower and with lower ultimate oil recovery.

As the result, the outcrop diatomitic rocks cannot be directly used as analogue material to study reservoir diatomite, since the outcrop diatomite contains only diatoms, and its permeability is much higher. In addition, the rock surface and liquid phases interact differently, i.e. the change in wettability occurs in different ways, especially due to the high content of clay minerals in the reservoir diatomite - kaolinite and illite, which make the rock surface less water-wet. Previous research on adsorption of polar organic components in crude oil onto sandstones of different mineralogy showed increased preference of the negatively charged clay minerals for positively charged nitrogen-containing bases at acidic pH [19]. However, since the outcrop diatomite from the Fur formation is a pure diatomitic rock, it can be used to study wettability and charge of the diatomitic surface in future adsorption tests, which will demonstrate the ability of diatomite to adhere the oil components onto its surface.

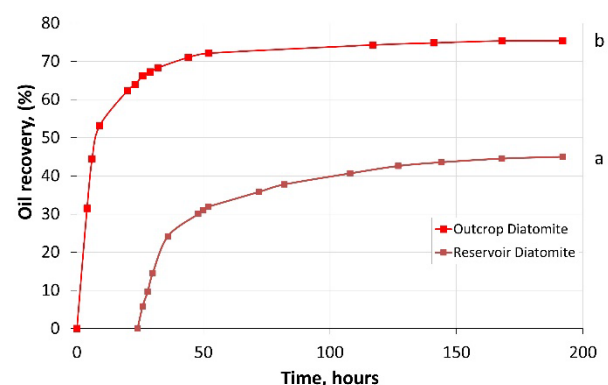


Fig. 5. SI oil recovery results of the reservoir (a) and outcrop (b) diatomite at ambient temperature using FW as the imbibing brine.

3.3 CO₂ storage

Diatomite deposits can be characterized as a unique geological formation consisting primarily of low-reactive and chemically stable silica, which, along with high porosity and large surface area, makes diatomite an attractive alternative for CO₂ storage projects. This section presents the results of experimental tests on the geochemical stability of the studied reservoir and outcrop rocks when exposed to carbonated water under reservoir conditions. The results may have implications for assessing the interaction of CO₂ with the porous diatomite matrix, which could potentially be reflected in dissolution and mineralization processes.

A series of carbonated LS exposure tests were performed on both reservoir and outcrop powdered material at 60 °C and 80 bar. The duration of the experiment was chosen to be 1 month on the basis that this

is a reasonable time to observe any chemical changes, given that the rock powder is mixed with a large volume of CW (≈ 2 wt% of solid phase), which significantly exceeds the rock/FW ratio in real reservoirs.

Figure 6 shows the changes in pH and concentrations of Na^+ , Cl^- and SO_4^{2-} ions in CLS over the course of a month of the exposure test. The results show minor variations in exposure brine pH throughout the test, with pH values around 5 for both reservoir diatomite and outcrop diatomite (Figure 6a). This indicates that there are no significant chemical changes in the CLS/rock system, confirmed by slight variations in ionic concentrations.

In the brine, minor appearances of Na^+ and Cl^- ions are observed, the relative concentration of which does not exceed 1.50 mM. These minor amounts of ions can be released from the surfaces of the rock samples (Figures 6b and 6c).

There is some dissolution of pyrite from the reservoir diatomite, and IC tests indicate approximately 0.9 mM SO_4^{2-} ions in the brine phase that was in contact with the reservoir diatomite sample. However, these changes are minor (Figure 6d).

Figures 7 and 8 show SEM images of reservoir and outcrop diatomite after the exposure tests. Visual assessment of the images does not indicate any changes in mineral structures compared to the original unexposed samples. The edges of the grains do not appear to be unclear or with precipitations, thus, CLS did not affect the integrity of the grains during the exposure tests under the selected test conditions.

The surface characterization analysis was complemented by EDX elemental composition measurements, Table 5. Minor changes in composition according to the EDX analysis were observed for both diatomite samples exposed to CLS. The Si level in the reservoir diatomite sample increased from 58.87 to 72.82% because of pyrite dissolution and difference of areas that were used for EDX measurements for non-exposed and exposed samples. However, the element content of the exposed reservoir diatomite sample demonstrates the same set of main elements, without new ones. Thus, there are no indications of the formation of new minerals on the surface of the rock.

As can be seen, most of the atomic weight percentages presented in Table 5 do not experience any significant change, confirming the low degree of geochemical reactions. The level of pH did not change significantly and fluctuated slightly within one pH unit. The pH level of the liquid from the cell with reservoir diatomite was around 5.3 during the tests, and the pH level of outcrop diatomite was around 4.8.

Thus, since diatomite samples are characterized by high porosity and exhibit high chemical stability and low changes during CLS exposure tests, the test material has significant potential for CO_2 storage.

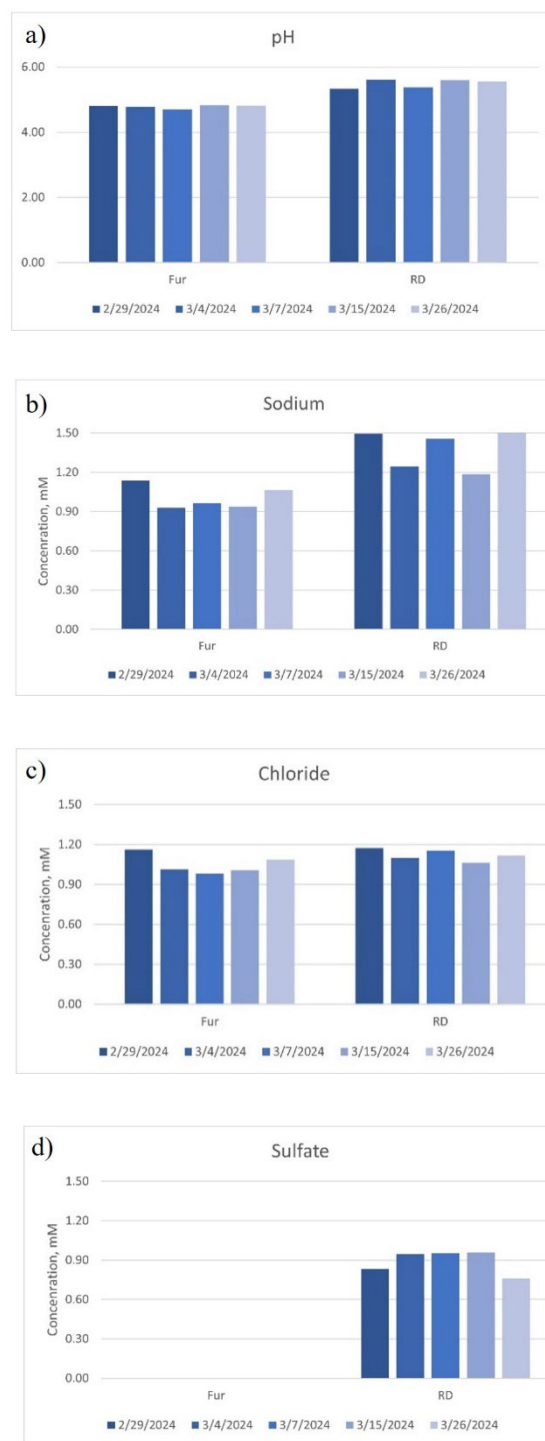


Fig. 6. The pH and IC results of CLS taken throughout the month of the exposure test.

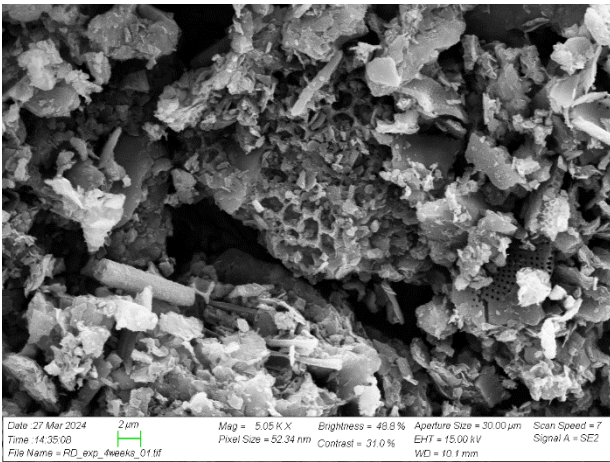


Fig. 7. SEM image of reservoir diatomite exposed to CLS at magnification 5500.

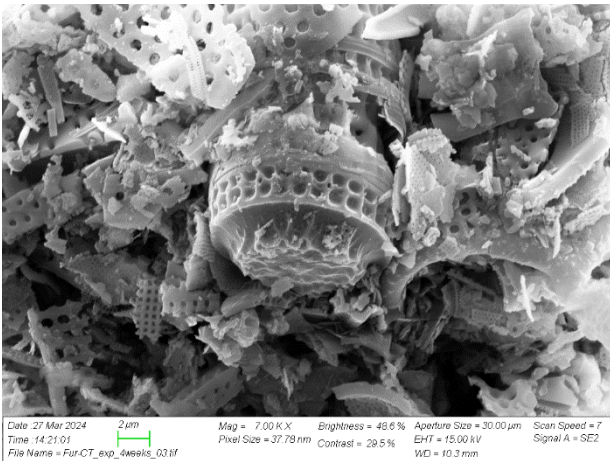


Fig. 8. SEM image of the outcrop Fur diatomite exposed to CLS at magnification 7000.

Table 5. Elemental composition (at. %) of reservoir and outcrop diatomite prior to and post exposure to CLS.

Elements	Reservoir diatomite		Outcrop diatomite	
	Non-exposed	Exposed	Non-exposed	Exposed
	(at. %)			
Na	1	0	0	0
Mg	1	1	0	0
Al	16	16	2	3
Si	59	72	98	97
S	5	1	0	0
K	9	5	0	0
Fe	9	5	0	0
Ca	0	0	0	0
Total	100	100	100	100

4 Conclusions

Better understanding of tight reservoir characteristics is an indispensable step in improving oil recovery and CO₂ storage missions. Besides low-permeability

sandstone, shale, and chalk, there is a less-studied reservoir rock – diatomite. The results of the current research provide improved understanding whether low-emission solutions, such as water-based EOR-methods, are applicable and whether diatomitic reservoirs are good reservoir rocks for CO₂ storage.

Spontaneous imbibition tests showed a great potential for diatomite oil recovery with water based EOR solutions because of the presence of strong capillary forces facilitating spontaneous uptake of water into the rock. The spontaneous imbibition tests showed that the outcrop sample was clearly on the water wet side, spontaneously imbibing water, and that the capillary forces mobilized the oil to reach a recovery of 75 %OOIP. However, the reservoir diatomite was found to be mixed-wet because of high clay minerals content shown by XRD (illite-kaolinite) and SEM images (diatom frustules are surrounded with clay minerals – Figure 3). The oil production plateau reached the value of about 45 %OOIP. These findings demonstrate the significance of capillary forces, highlighting the necessity to consider them when assessing the ultimate recovery potential from reservoirs in laboratory experiments or when conducting modeling and simulations of fluid flow within reservoirs.

Exposure tests with carbonated low-salinity water did not show significant changes in rock composition after 1 month, and only minor dissolution of pyrite was noticed. Thus, due to the high porosity and a limited reactive surface, diatomite seems to be a good option for CO₂ storage purposes.

The next step of the study is designing Smart Water for inducing wettability alteration toward more water wet conditions for improved displacement of oil from diatomite reservoirs.

The authors acknowledge the Research Council of Norway and the industry partners of NCS2030 – RCN project number 331644 – for their support.

References

1. NPD’s resource report 2019 (including the challenging barrels from tight reservoirs): <https://www.npd.no/globalassets/1- npd/publikasjoner/ressursrapport-2019/resource-report-2019.pdf>
2. H. Hermansen, G. H. Landa, J. E. Sylte, L. K. Thomas. *J. Pet. Sci. Eng.*, **26**(1-4), 11-18 (2000).
3. N. J. Wallace, E. D. Pugh. *cSPE Ann. Tech. Conf. Exhib.*, **SPE-26626** (1993).
4. P. R. Perri, M. A. Emanuele, W. S. Fong, M. F. Morea. In *SPE West. Reg. Meet.*, **SPE-62526** (2000).
5. P. R. Perri, J. Cooney, B. Fong, D. Julander, A. Marasigan, M. Morea, S. Heisler. *Class III (No. DOE/BC/14938-15)*. National Energy Technology Lab. (NETL), Tulsa, OK (United States). National Petroleum Technology Office (NPTO) (2000).
6. S. Akin, J. M. Schembre, S. K. Bhat, A. R. Kavscek. *J. Pet. Sci. Eng.*, **25**(3-4), 149-165 (2000).

7. D. Frydas. *Revue de Micropaléontologie*, **49**(2), 86-96 (2006).
8. I. D. P. Torrijos, T. Puntervold, S. Strand, P. Aslanidis, I. Fjelde, A. Mamonov. The National IOR Centre of Norway 2021 Report Number: **110** (2021).
9. U. Korsbech, H. K. Aage, B. L. Andersen, K. Hedegaard, N. Springer. *SPE Reservoir Eval. Eng.*, **9**(03), 259-265 (2006).
10. E. Amott. *Trans. AIME*, **216**(01), 156-162 (1959).
11. M. Fani, S. Strand, T. Puntervold, A. Mamonov, I. D. P. Torrijos, M. A. I. Khan. *Gas Sci. Eng.*, **205246** (2024).
12. K. S. Lee, J. H. Lee. *Gulf Professional Publishing* (2019).
13. Z. Aghaeifar, S. Strand, T. Austad, T. Puntervold, H. Aksulu, K. Navratil, S. Storås, D. Håmsø. *Energy & Fuels*, **29**(8), 4747-4754 (2015).
14. T. Puntervold, S. Strand, A. Mamonov, I. D. T. Piñerez. *Gulf Professional Publishing*. 109-184 (2023).
15. T. Puntervold, A. Mamonov, I. D. Piñerez Torrijos, S. Strand. *Energy & Fuels*, **35**(7), 5738-5747 (2021).
16. W. G. Anderson. *J. Pet. Technol.*, **38**(10), 1125-1144 (1986).
17. J. M. Schembre, S. Akin, L. M. Castanier, A. R. Kovsky. In *SPE West. Reg. Meet.* **SPE-46211** (1998).
18. T. Puntervold, A. Mamonov, Z. Aghaeifar, G. O. Frafjord, G. M. Moldestad, S. Strand, T. Austad. *Energy & Fuels*, **32**(7), 7374-7382 (2018).
19. A. Mamonov, P. Aslanidis, N. Fazilani, T. Puntervold, S. Strand, *Energy & Fuels*, **36**(18), 10785-10793 (2022).